Flexible SIW humidity sensors based on nanodiamond sensing films

Chang-ming Chen[1] (iD), Lu Chen[2], Yao Yao[3] and Ye Peng[1]

[1]College of Communication Engineering, Chengdu University of Information Technology, Chengdu 610225, China; [2]Engineering Practice Center, Chengdu Aeronautic Polytechnic, Chengdu 610100, China and [3]School of Automation Engineering, University of Electronic Science and Technology of China, Chengdu 610054, China

Abstract

In this paper, flexible substrate integrated waveguide (SIW) resonators have been designed and fabricated on polyimide substrates for humidity sensing applications. The proposed SIW resonant cavity allows the resonator to obtain the maximum humidity sensitivity and meet the demand for flexible microwave sensing detection. Meanwhile, the humidity response performance can be further significantly enhanced by introducing nanodiamond (ND) sensing material. Three prototypes of ND-coated SIW sensors with different bending radii are measured to analyze their humidity sensing performance. The experimental results demonstrate that the proposed ND-coated SIW sensor with the minimum bending radius can achieve a maximum humidity sensitivity of 1.09 MHz/% relative humidity (RH) in the high RH region (>75.3% RH) and a low humidity hysteresis of 1.8% in the range of 11.3–97.3% RH. This study provides a promising candidate to realize flexible microwave sensors with excellent sensing performance.

CAMBRIDGE UNIVERSITY PRESS

Introduction

Microwave and radio frequency sensors have been successfully designed for humidity monitoring applications, that address material moisture content, the food industry, environmental detection, health care and intelligent packaging [1–6]. These sensors provide a robust, real-time and nondestructive measurement platform for passive microwave sensing. In particular, compared with single resonator sensors, differential microwave sensors can mitigate the effects of cross-sensitivity caused by environmental factors and can thus provide higher detection accuracy and sensitivity [7–9]. However, because differential sensors have two relatively independent resonators, this may lead to complex and bulky sensors. Recently, substrate integrated waveguide (SIW)-based resonators are being considered for compact microwave humidity sensors due to their merits of compact size, simple manufacturing process, low radiation loss, high humidity sensing performance and good stability [10–12]. In [13, 14], SIW-based resonators with simple structures were demonstrated to achieve a good humidity response by introducing a sensitive region inside the cavity in a certain humidity range. To further reduce the dimensions of the sensors, half-mode SIW and quarter-mode SIW structures were used to achieve miniaturization while maintaining excellent humidity sensing performance [15, 16]. Nevertheless, these abovementioned SIW-based sensors are fabricated on rigid substrates such as RO4350, ceramics and Teflon, which constrains their applications in sensing fields where the geometric shapes of the materials under test are not flat. For instance, in the context of real-time monitoring of the relative humidity (RH) level of human skin or the ambient humidity surrounding the human body, the potential applications would involve the evaluation of human physiological health conditions. Split ring resonator-based pressure sensor arrays are successful examples of flexible microwave sensors that can be applied to human health monitoring [17]. In other applications, such as the early detection of coating breaches in steel pipelines, flexible sensors are also required to conform with the geometrical cylindrical structure [18]. These studies have provided valuable guidance for the design of high-performance flexible microwave sensors.

It is well known that a substrate with flexible mechanical properties is a key component for fabricating flexible microwave sensors. Several flexible substrates including paper [19, 20], liquid crystal polymer [21, 22], polyimide (PI) [23, 24], and polyethylene terephthalate (PET) [25, 26] have been successfully developed into flexible antennas with good performance. Among these materials, PI possesses excellent RF characteristics and low dissipation factors [27, 28], so it has become a candidate substrate for the design of microwave humidity sensors [29, 30]. However, in these works, the effects of bending behaviors on the humidity sensing performance have not been systematically studied. Moreover, to date, few researchers have investigated PI-based compact flexible SIW humidity sensors.

On the other hand, humidity sensors are usually integrated with sensing material to achieve high sensitivity. From this perspective, a variety of humidity sensing material including zero-dimensional fullerenes (C_{60}) [31], carbon nanotubes [32], nanodiamonds (NDs) [33] and graphene oxide [34, 35] have been successfully employed to implement impedance-type or capacitance-type humidity sensors at low frequencies. ND, which is regarded as a functional nanocarbonaceous material, has recently gained increasing interest for the fabrication of humidity and gas sensors due to its excellent electronic, water adsorption capacity and chemical properties [36, 37]. ND provides a high Young's modulus, large surface area and rich surface groups (carboxyl and hydroxyl groups) [38]. This makes it a particularly promising and attractive sensing material for environmental monitoring applications. For example, Ahmad *et al.* investigated gas sensing characteristics by coating ND films on a silicon cantilever array; the gas chemisorption of ND films then resulted in an increase in its mass, accordingly changing the resonant frequency of the sensor [39]. In 2014, Yao *et al.* designed novel QCM humidity sensors using ND material as sensing films and found that the ND-coated humidity sensors exhibited outstanding humidity response owing to the large specific surface area of NDs in the presence of water molecule adsorption [40]. More recently, a flexible wearable humidity sensor with ND sensing films has been demonstrated highly sensitive characteristics [41]. However, it is worth noting that most of the ND-coated sensors studied in the literature operated under either low resonant frequencies or direct current (DC) conditions. To the best of our knowledge, few works have developed flexible SIW-based humidity sensors based on ND sensing materials.

Herein, we propose a high-sensitivity and low-humidity hysteresis flexible SIW humidity sensor using NDs as sensing films in the C-band frequency range. Using simple printed circuit board (PCB) processes, three humidity sensor prototypes with different bending radii are fabricated on PI substrates, and their humidity sensing properties are comparatively analyzed and discussed.

Theory and design

Figure 1(a) shows the planar geometrical structure of the proposed microwave humidity sensor. It consists of an SIW cavity with a feeding microstrip line, a rectangular patch, and a U-shaped slot that is etched on the top metal layer. The substrate is PI with ε_r = 3.5 and tan δ = 0.0009, and the thickness is 0.13 mm. The length and width of the SIW cavity can be determined based on the design theory of SIWs [42]. To ensure that the resonator can obtain the best S_{11} and have the strongest electric field distribution in the sensing region, the length l_2 of the rectangular patch, the width w_2 of the rectangular patch, and the depth l_1 of the U-shaped slot are carefully optimized by using high frequency structure simulator tools. The reflection parameters of the resonator are mainly affected by l_2 and w_2. Figures 1(b) and 1(c) shows the frequency curves with different lengths l_2 and w_2. These figures show that when the optimal values of l_2 and w_2 are 2.3 and 4.6 mm, respectively, the magnitude of S_{11} reaches the maximum value. Since the loss of the resonator can be characterized by S_{11}, the optimal geometric size of the sensor at a resonant frequency of 7.5 GHz can be obtained by comparing the S_{11} of the corresponding simulated curves. Table 1 lists the general physical parameters of the proposed resonator. Figure 1(d) also displays the simulated vector curves of the electric field distribution of the SIW cavity at 7.5 GHz. The electric field is mainly concentrated in the metal patch region, indicating

that the patch region is the best geometric location for depositing the sensing films to enhance the humidity response, as shown in the dotted box in Fig. 1(a).

The proposed structure can be regarded as an SIW resonator with a slot. Its central resonant frequency can be approximately expressed as [42]

$$f_{\text{res}} = \frac{c_0}{2L_{eff}\sqrt{\varepsilon_{eff}}} \qquad (1)$$

where L_{eff} represents the effective resonance length of the resonator, ε_{eff} is the effective dielectric constant and c_0 is the light velocity in vacuum. In this design, L_{eff} is mainly determined by l_1 and l_2, while the ε_{eff} of equation (1) is given by [4]

$$\varepsilon_{eff} = 1 + q_{PI}(\varepsilon_{r,PI} - 1) + q_{ND}(\varepsilon_{r,ND} - 1) \qquad (2)$$

where q_{PI} and q_{ND} represent the partial filling factors of the PI and ND material, respectively. They are closely associated with the thickness of the sensing films, the substrate, the dimensions of the U-shaped slot, and the length (l_2) and width (w_2) of the sensing region. The coefficients $\varepsilon_{r,PI}$ and $\varepsilon_{r,ND}$ are the relative permittivity of the substrate and the ND films, respectively.

Equation (2) reveals that the effective dielectric constant ε_{eff} is determined by $\varepsilon_{r,PI}$ when the sensing region is not filled with any sensing material. Therefore, the electromagnetic characteristics of the resonator rely on the dielectric properties of the air surrounding the resonator. When the ND films are coated on the sensing region, due to the PI substrate's insensitivity to humidity [41], ε_{eff} will strongly depend on the dielectric properties of the ND films ($\varepsilon_{r,ND}$) in the case of humidity change. Obviously, the presence of the ND material within the sensing region will increase the effective dielectric constant. Thereafter, any change in $\varepsilon_{r,ND}$ will be translated to a change in f_{res} according to equation (1). Due to their hydrophilic character, the ND material induces a change in $\varepsilon_{r,ND}$ as a function of humidity. As a result, electromagnetic waves traveling through the resonator will be influenced as a function of humidity. Under the excitation of electromagnetic fields, water molecules attached to sensing materials will adsorb electromagnetic energy and show the polarization phenomenon. Accordingly, the dielectric properties of the water molecules will change with the variation in moisture, which are reflected by ε_{eff} in equation (2). Based on these principles, the proposed SIW resonator can be used to detect humidity variations around the cavity with microwave parameters.

As shown in Figs 2(a)–2(c), three prototypes of resonators with different bending radii are fabricated to investigate their electromagnetic properties. For simplicity, we define the bending radius of the resonator as R. For the flat resonator, the bending radius can be expressed as R = ∞. We bent the fabricated resonator until the radius reached a minimum of 19.74 mm (the moment when the SMA connector nearly touches the other end of the PCB). Therefore, the radius range of the bending test is 1.5 mm to ∞. Three resonators with bending radii of R = ∞, 39.47 and 19.74 mm are labeled as sensors A, B, and C. To accurately display the bending radius of the sensor, sensors B and C are mounted on two foam cylinders corresponding to the bending radius. As shown in Figs 3(a) and 3(b), it is clear that the electric field intensity of the sensing region at 7.5 GHz decreases as the bending radius decreases. This means that the absorbed electromagnetic energy of the flexible resonators also decreases with the reduction of the bending radii.
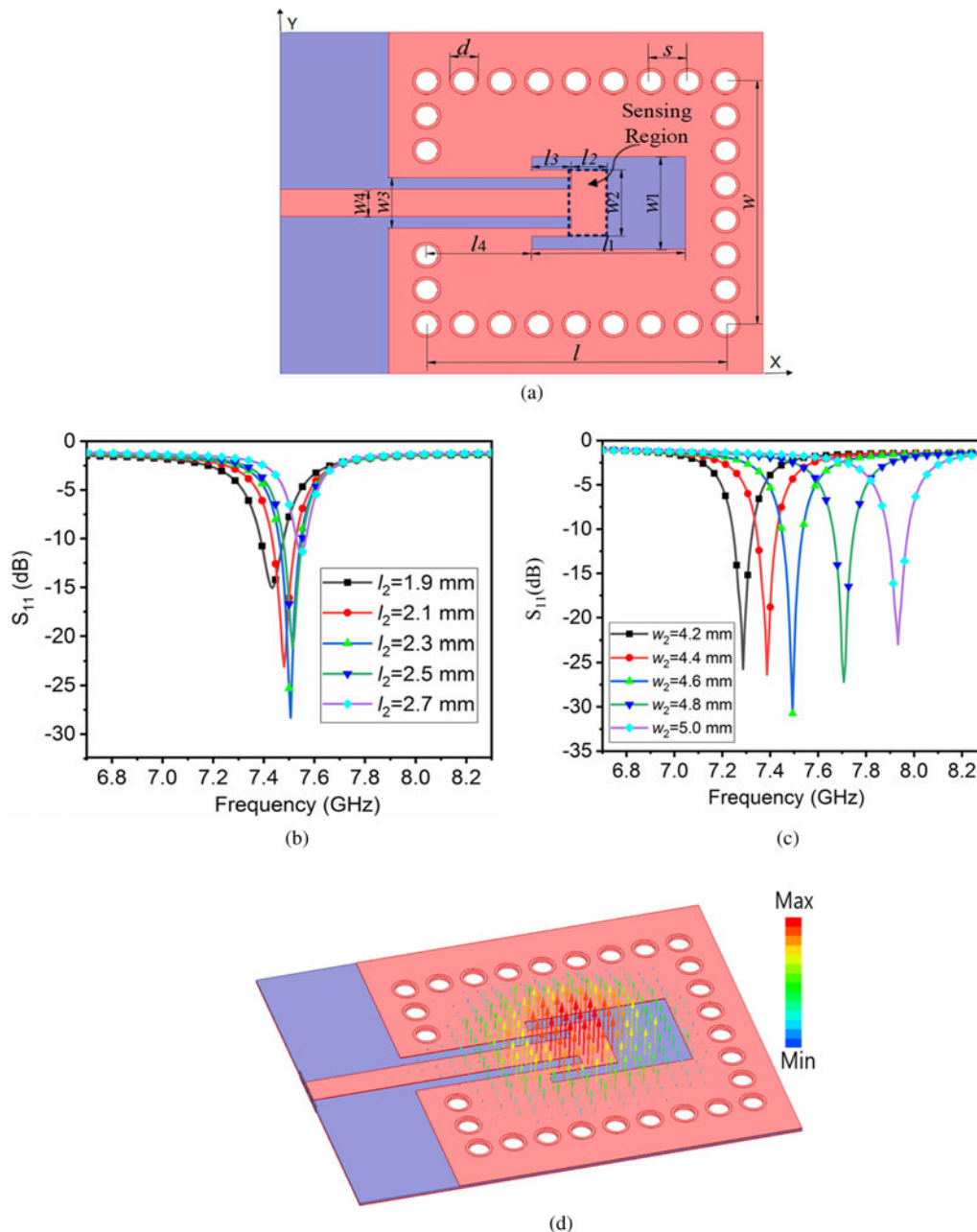
Figure 1. The proposed sensor model and the simulated results. (a) Structure of the SIW resonator. (b) The S_{11} with different length l_2 of the sensing region. (c) The S_{11} with different width w_2 of the sensing region. (d) The electronic field distribution of the cavity at 7.5 GHz.

The measured S_{11} values of the three resonators without sensing materials are plotted in Fig. 4. Examination of this figure clearly shows that the resonant frequencies of the resonators increase with decreasing bending radius. As reported in [43], this can be attributed to the fact that the bending strip line affects the resonator's effective resonance length. The greater the resonator is bent, i.e. around a smaller bending radius, the greater the effective resonance length is reduced, and thus, the resonant frequencies are shifted up according to equation (1).

Humidity measurement

A commercial colloidal suspension of ND (1 mg/ml) was purchased from Nanjing Xianfeng Nano Co. Ltd., China. Seven microliters of ND solution was coated on the sensing region of the cavity by using a drop-coating process. Then, the three prototypes of sensors were naturally dried for two hours at room temperature. Figure 5 shows a field-emission scanning electron microscopy (FESEM, Hitachi S-4800) image of the ND films. The surface morphology of the ND is granular, and the particle size is ~10 nm. These small particles are characterized by a large surface area and surface state densities. This is beneficial for enhancing the humidity sensing performance.

A schematic diagram of the overall experimental setup is shown in Fig. 6. For the convenience of testing, sensors B and C were kept in the bending state but with the foam cylinder removed. The scattering parameters of the sensors were measured using a vector network analyzer (N5244A, Agilent). Saturated

Table 1. The general physical parameters of the proposed resonator

Parameters	Values (mm)	Parameters	Values (mm)	Parameters	Values (mm)
l	19.3	w	16.8	l_1	9.8
l_2	2.3	l_3	2.6	l_4	6.7
w_1	6.4	w_2	4.6	w_3	3.5
w_4	1.9	s	2.4	d	0.9

LiCl, MgCl$_2$, Mg(NO$_3$)$_2$, NaCl, KCl, and K$_2$SO$_4$ solutions at room temperature were used to provide approximately 11.3, 32.8, 54.3, 75.3, 84.3 and 97.3% RH environment levels, respectively. First, the humidity characteristics of three sensors without sensing materials were tested. We found that the sensors had almost no humidity response, and the measured results were consistent with those shown in Fig. 4. This further confirms that the PI substrate is insensitive to moisture. Therefore, we only investigated the humidity performance of the sensors using ND sensing films in this work. To ensure the repeatability of the humidity response measurement, each fabricated sensor was continuously carried out for three days, and the measured data were recorded under the same experimental conditions.

Results and discussion

Figure 7 plots the measured resonant frequency shift curves of the three sensors with the ND material as a function of RH. The resonant frequency of each sensor shifts toward a lower frequency with increasing RH levels accordingly. These measurements show that the frequency shift depends closely on the humidity adsorption properties of the ND-sensitive films. These features can be attributed to the increase in the dielectric permittivity of the ND, which is caused by the adsorption of a large number of water molecules in the ND sensing films [44], resulting in an increase in the effective dielectric constant (ε_{eff}). According to equation (1), the resonance frequency, f_{res}, will decrease with increasing RH levels.
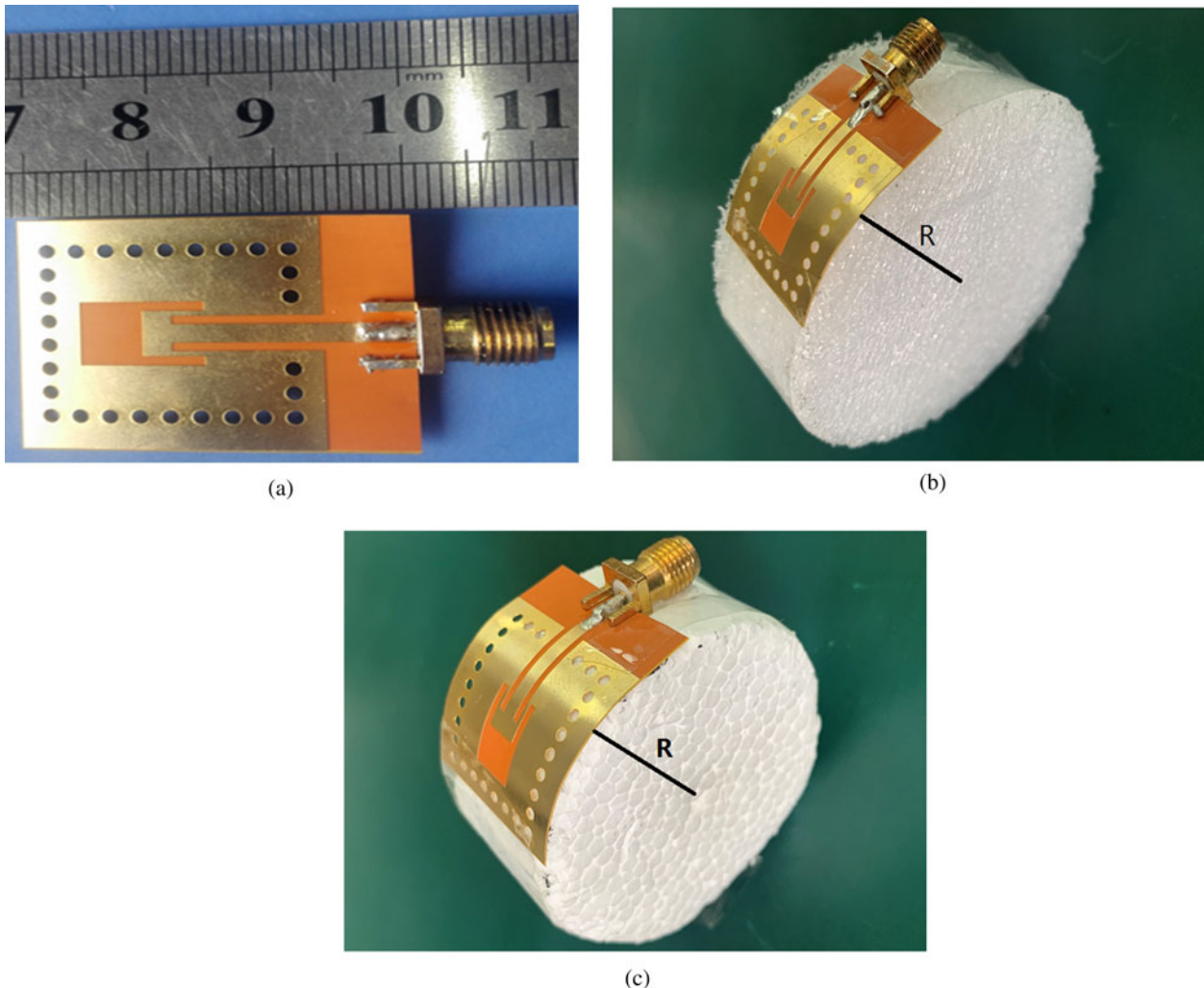
Figure 2. The photographs of the fabricated sensors with different radii. (a) Sensor A ($R = \infty$). (b) Sensor B ($R = 39.47$ mm). (c) Sensor C ($R = 19.74$ mm).
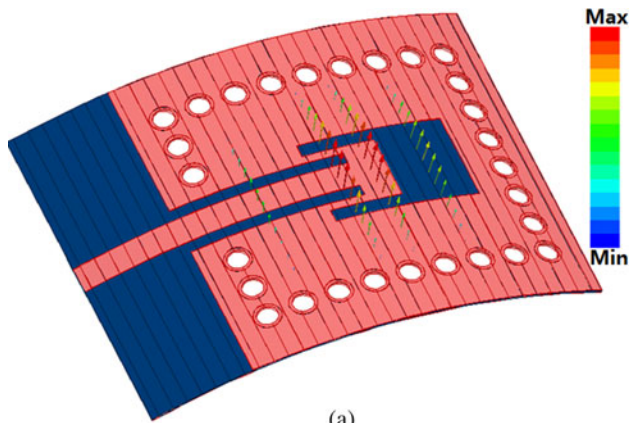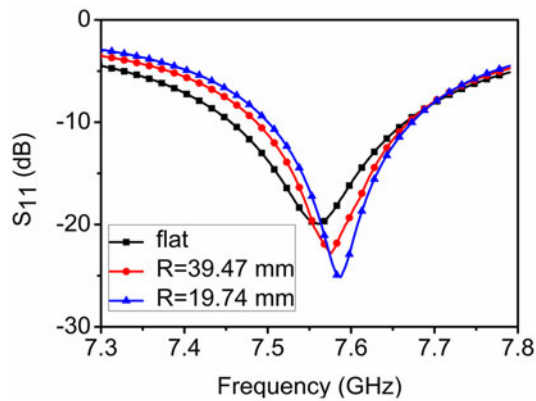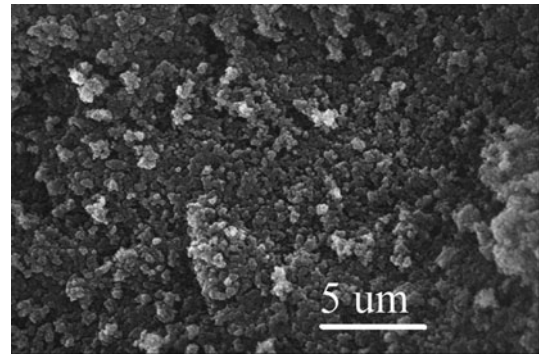
(a)
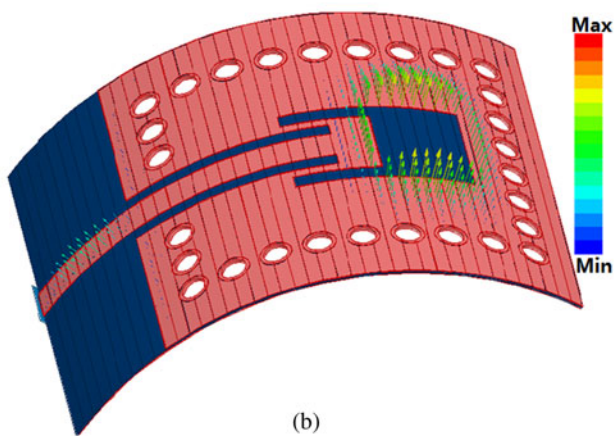
(b)

Figure 3. The simulated electronic field distribution of the bending sensors at 7.5 GHz. (a) Sensor B. (b) Sensor C.
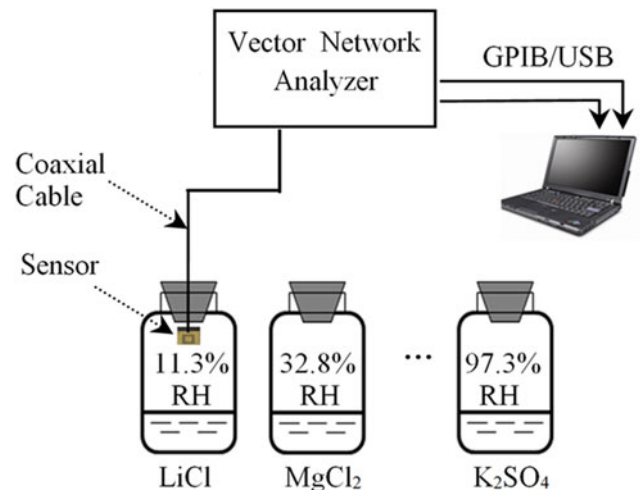

Figure 5. The SEM image of the ND films.

Figure 6. Humidity experimental setup.

Figure 4. The measured S_{11} of the fabricated three sensors.

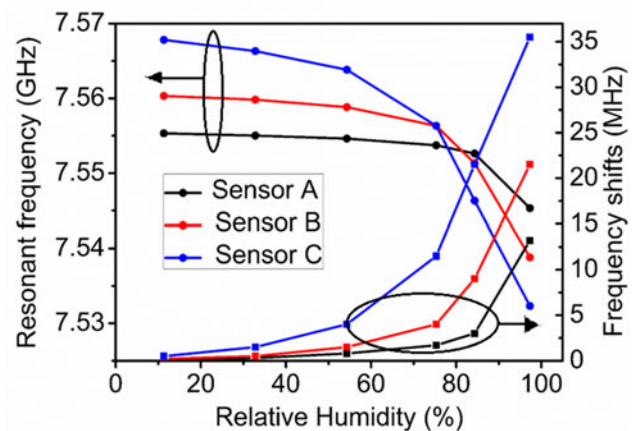**Figure 7.** Measured resonant frequency shifts of the three sensors at different humidity levels.

Figure 7 also shows that in the range of 11.3–97.3% RH, the maximum frequency shift values of sensors A, B, and C are approximately 10, 21.5, and 35.5 MHz, respectively. Obviously, the frequency shifts of sensors B and C are larger than that of sensor A. We can calculate that sensor C obtains the largest humidity sensitivity of 172 kHz/%RH from 11.3 to 75.3% RH and 1.09 MHz/%RH in the RH range of 75.3–97.3%. These results indicate that the humidity sensitivity of the fabricated sensors can be significantly enhanced by reducing the resonator's bending radius

under the limitation that the bending radius of the substrate can reach the minimum value. The possible reasons can be explained as follows: the interspaces between ND particles will expand due to the stretching of the bending sensing films, thus forming wider sensing channels [41]. Among the three sensors, sensor C with the smallest bending radius can absorb more

Figure 8. Measured S_{11} of the fabricated sensors as a function of humidity.

that the measured maximum loss of sensor C is −2.34 dB, which indicates that the ND-based flexible sensor only introduces a small dielectric loss to obtain a large humidity response. These results suggest that the proposed resonators are more suitable to operate under flexible conditions.

To examine the humidity hysteresis characteristics, the three fabricated sensors first carried out a series of RH points from low to high for water molecule adsorption and then from a high to low RH environment for water molecule desorption. At each RH point, we recorded the stable frequency shift values of the sensors. Figure 9 plots the humidity hysteresis curves of the three sensors with 7 µl of deposited ND suspension. This figure shows that the humidity hysteresis of sensors A, B and C are approximately 0.23, 0.93 and 1.8% RH, respectively. The possible causes for this phenomenon are as follows: the water molecules surrounding the sensors are mainly adsorbed on the surface of the ND films due to the good hydrophilicity of the ND material [38]. As reported in the literature [45], water molecules will vibrate violently under high-frequency electromagnetic field excitation. As illustrated in Figs 1(d), 3(a) and 3(b), the sensing region of sensor A has the strongest electric fields. Therefore, water molecules on the sensing films will obtain enough electromagnetic energy to achieve a fast dynamic equilibrium of adsorption and desorption. Compared with sensors A and B, although sensor C has a slightly larger humidity hysteresis, it is still superior to the values of ND-coated humidity sensors operating under low-frequency or DC conditions [40, 41].

A comparison between the fabricated flexible SIW sensor with ND sensing films and previous SIW humidity research works is
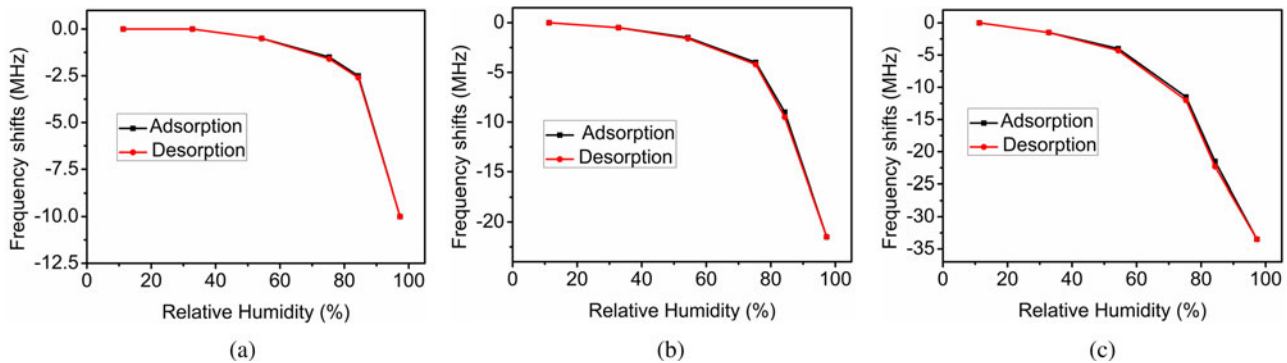
water molecules to diffuse through the sensing films due to the largest interspaces and the widest channels between ND particles, thus producing a higher frequency shift than that of sensors A and B. These experimental results demonstrate that the humidity response performance of the sensors can be effectively improved by coating ND sensing films, and the flexible SIW structure can significantly enhance the humidity sensitivity of the sensors.

Figure 8 displays the variation in S_{11} with RH for the three sensors. The magnitude of S_{11} of each sensor decreases with increasing humidity. This means that the electromagnetic energy loss of the resonator increases as the humidity level increases. We note

Figure 9. The humidity hysteresis. (a) Sensor A. (b) Sensor B. (c) Sensor C.

Table 2. Comparison of other SIW humidity sensors in the literature

Refs.	Structure	RH range (%)	Flexible sensor	Sensitive material	Normalized sensitivity (%/%RH)
[10]	SIW resonator	11–97	No	Yes	5.41×10^{-3}
[11]	SIW resonator	20–85	No	No	15.8×10^{-3}
[12]	Double-folded SIW resonator	30–80	No	No	6.27×10^{-3}
[13]	SIW resonator	0–80	No	No	2.43×10^{-3}
[14]	SIW interferometer	20–70	No	No	0.86×10^{-3}
[15]	Half-mode SIW resonator	11.3–97.3	No	Yes	13.3×10^{-3}
[16]	Quarter-mode SIW resonator	0–80	No	No	0.61×10^{-3}
This work	SIW resonator	11.3–97.3	Yes	Yes	14.5×10^{-3}

presented in Table 2. Considering that the operating frequency of each sensor may be different, we normalized the sensitivity of the sensors to ensure fair comparisons. Notably, the air-filled SIW sensor in reference [11] shows the highest sensitivity but has a narrow range of RH responses. Compared with most of these reported SIW humidity sensors, our SIW sensors exhibit the merits of flexibility, high humidity sensitivity, wide humidity response range and low fabrication cost.

Conclusion

In this work, flexible SIW resonators have been proposed for humidity monitoring applications. Three kinds of humidity sensors using ND sensing material are fabricated on a PI substrate, and their humidity sensing characteristics are comparatively investigated and discussed. The experimental results demonstrate that the proposed SIW resonator can provide the flexible sensor with the best humidity sensitivity, and the introduction of ND sensing material can significantly enhance the sensor's humidity response. This study provides a promising candidate to implement a high-sensitivity flexible microwave humidity sensor. Moreover, this research also indicates the potential applications of the proposed flexible SIW sensor for human health monitoring or other nonplanar material dielectric property detection.

Author contributions. Chang-ming Chen: conceptualization, data curation, funding acquisition, and writing & editing. Lu Chen: investigation, data curation. Yao Yao: formal analysis. Peng Ye: formal analysis.

Conflict of interest. The authors declare no conflict of interest.

References

1. **Virtanen J, Ukkonen L, Björninen T, Elsherbeni AZ and Sydänheimo L** (2011) Inkjet-printed humidity sensor for passive UHF RFID systems. *IEEE Transactions on Instrumentation and Measurement* **60**, 2768–2777.
2. **Amin EM, Bhuiyan MS, Karmakar NC and Winther-Jensen B** (2014) Development of a low cost printable chipless RFID humidity sensor. *IEEE Sensors Journal* **14**, 140–149.
3. **Kim YH, Jang K, Yoon YJ and Kim YJ** (2006) A novel relative humidity sensor based on microwave resonators and a customized polymeric film. *Sensors and Actuators B* **117**, 315–322.
4. **Eyebe GA, Bideau B, Boubekeur N, Loranger É and Domingue F** (2017) Environmentally-friendly cellulose nanofibre sheets for humidity sensing in microwave frequencies. *Sensors and Actuators B* **245**, 484–492.
5. **Eyebe GA, Bideau B, Loranger É and Domingue F** (2019) TEMPO-oxidized cellulose nanofibre (TOCN) films and composites with PVOH as sensitive dielectrics for microwave humidity sensing. *Sensors and Actuators B: Chemical* **291**, 385–393.
6. **Feng Y, Xie L, Chen Q and Zheng LR** (2015) Low-cost printed chipless RFID humidity sensor tag for intelligent packaging. *IEEE Sensors Journal* **15**, 3201–3208.
7. **Ebrahimi A, Scott J and Ghorbani K** (2018) Transmission lines terminated with LC resonators for differential permittivity sensing. *IEEE Microwave Wireless Components Letters* **28**, 1149–1151.
8. **Ebrahimi A, Tovar-Lopez FJ, Scott J and Ghorbani K** (2020) Differential microwave sensor for characterization of glycerol–water solutions. *Sensors and Actuators B: Chemical* **321**, 1–7.
9. **Vélez P, Muñoz-Enano J and Martín F** (2019) Differential sensing based on quasi-microstrip mode to slot-mode conversion. *IEEE Microwave Wireless Components Letters* **29**, 690–692.
10. **Chen CM, Xu J and Yao Y** (2017) SIW resonator humidity sensor based on layered black phosphorus. *Electronics Letters* **53**, 249–251.
11. **Ndoye M, Kerroum I, Deslandes D and Domingue F** (2017) Air-filled substrate integrated cavity resonator for humidity sensing. *Sensors and Actuators B: Chemical* **252**, 951–955.
12. **Wei Z, Huang J, Li J, Li J, Liu X and Ni X** (2019) A compact double-folded substrate integrated waveguide re-entrant cavity for highly sensitive humidity sensing. *Sensors* **19**, 1–12.
13. **Matbouly HE, Boubekeur N and Domingue F** (2015) Passive microwave substrate integrated cavity resonator for humidity sensing. *IEEE Transaction on Microwave Theory Techniques* **63**, 4150–4156.
14. **Benleulmi A, Boubekeur N and Massicotte D** (2019) A highly sensitive substrate integrated waveguide interferometer applied to humidity sensing. *IEEE Microwave Wireless Components Letters* **29**, 68–70.
15. **Chen CM, Xu J and Yao Y** (2018) Fabrication of miniaturized CSRR-loaded HMSIW humidity sensors with high sensitivity and ultra-low humidity hysteresis. *Sensors and Actuators B: Chemical* **256**, 1100–1106.
16. **Jones TR, Zarifi MH and Daneshmand M** (2017) Miniaturized quarter-mode substrate integrated cavity resonators for humidity sensing. *IEEE Microwave Wireless Components Letters* **27**, 612–614.
17. **Dijvejin ZA, Kazemi KK, Zarasvand KA, Zarifi MH and Golovin K** (2020) Kirigami-enabled microwave resonator arrays for wireless, flexible, passive strain sensing. *ACS Applied. Materials & Interfaces* **12**, 44256–44264.
18. **Zarifi MH, Deif S, Abdolrazzaghi M, Chen B, Ramsawak D, Amyotte M, Vahabisani N, Hashisho Z, Chen W and Daneshmand M** (2018) A microwave ring resonator sensor for early detection of breaches in pipeline coatings. *IEEE Transaction on Industrial Electronics* **65**, 1626–1635.
19. **Li X, Wang YH, Lu A and Liu X** (2015) Controllable hydrothermal growth of ZnO nanowires on cellulose paper for flexible sensors and electronics. *IEEE Sensors Journal* **15**, 6100–6107.
20. **Ullah MA, Islam MT, Alam T and Ashraf FB** (2018) Paper-based flexible antenna for wearable telemedicine applications at 2.4 GHz ISM band. *Sensors* **18**, 1–13.
21. **Kao HL, Cho CL, Zhang XY, Chang LC, Wei BH, Dai X and Chiu HC** (2014) Bending effect of an inkjet-printed series-fed two-dipole antenna on a liquid crystal polymer substrate. *IEEE Antennas and Wireless Propagation Letters* **13**, 1172–1175.
22. **Jilani SF, Munozc MO, Abbasi QH and Alomainy A** (2019) Millimeter-wave liquid crystal polymer based conformal antenna array for 5G applications. *Antennas and Wireless Propagation Letters* **18**, 84–88.
23. **Peng JJ, Qu SW, Xia M and Yang S** (2020) Wide-scanning conformal phased array antenna for UAV radar based on polyimide film. *Antennas and Wireless Propagation Letters* **19**, 1581–1585.
24. **Russell C, Swithenbank M, Wood CD, Burnett AD, Li L, Linfield EH, Davies AG and Cunningham JE** (2016) Integrated on-chip THz sensors for fluidic systems fabricated using flexible polyimide films. *IEEE Transactions on Terahertz Science and Technology* **6**, 619–624.
25. **Guo X, Hang Y, Xie Z, Wu C, Gao L and Liu C** (2017) Flexible and wearable 2.45 GHz CPW-fed antenna using inkjet-printing of silver nanoparticles on PET substrate. *Microwave and Optical Technology Letters* **59**, 204–208.
26. **Castro AT and Sharma SK** (2018) Inkjet-printed wideband circularly polarized microstrip patch array antenna on a PET film flexible substrate material. *Antennas and Wireless Propagation Letters* **17**, 176–179.
27. **Wang Z, Qin L, Chen Q, Yang W and Qu H** (2019) Flexible UWB antenna fabricated on polyimide substrate by surface modification and *in situ* self-metallization technique. *Microelectronic Engineering* **206**, 12–16.
28. **McGibney E, Barton J, Floyd L, Tassie P and Barrett J** (2011) The high frequency electrical properties of interconnects on a flexible polyimide substrate including the effects of humidity. *IEEE Transactons on Components Packaging and Manufacturing Technology* **1**, 4–15.
29. **Chang K, Kim YH, Kim YJ and Yoon YJ** (2007) Functional antenna integrated with relative humidity sensor using synthesised polyimide for passive RFID sensing. *Electronics Letters* **43**, 256–260.
30. **Salas-Sánchez AÁ, López-Martín ME, Rodríguez-González JA and Ares-Pena FJ** (2017) Design of polyimide-coated Yagi-Uda antennas for monitoring the relative humidity level. *IEEE Geoscience and Remote Sensing Letters* **14**, 961–963.

31. **Radeva E, Georgiev V, Spassov L, Koprinarov N and Kanev S** (1997) Humidity adsorptive properties of thin fullerene layers studied by means of quartz micro-balance. *Sensors and Actuators B: Chemical* **42**, 11–13.

32. **Su PG and Tsai JF** (2009) Low-humidity sensing properties of carbon nanotubes measured by a quartz crystal microbalance. *Sensors and Actuators B: Chemical* **135**, 506–511.

33. **Yao Y and Xue Y** (2015) Impedance analysis of quartz crystal microbalance humidity sensors based on nanodiamond/graphene oxide nanocomposite film. *Sensors and Actuators B: Chemical* **211**, 52–58.

34. **Yuan Z, Tai H, Ye Z, Liu C, Xie G, Du X and Jiang Y** (2016) Novel highly sensitive QCM humidity sensor with low hysteresis based on graphene oxide (GO)/poly(ethyleneimine) layered film. *Sensors and Actuators B: Chemical* **234**, 145–154.

35. **Kuznetsova IE, Anisimkin VI, Kolesov VV, Kashin VV, Osipenko VA, Gubin SP, Tkachev SV, Verona E, Sun S and Kuznetsova AS** (2018) Sezawa wave acoustic humidity sensor based on graphene oxide sensitive film with enhanced sensitivity. *Sensors and Actuators B: Chemical* **272**, 236–242.

36. **Ahmad RK, Parada AC and Jackman RB** (2011) Nanodiamond-gated silicon ion-sensitive field effect transistor. *Applied Physics Letters* **98**, 153507-1–153507-3.

37. **Williams OA, Nesladek M, Daenen M, Michaelson S, Hoffman A, Osawa E, Haenen K and Jackman RB** (2008) Growth, electronic properties and applications of nanodiamond. *Diamond & Related Materials* **17**, 1080–1088.

38. **Mochalin VN, Shenderova O, Ho D and Gogotsi Y** (2012) The properties and applications of nanodiamonds. *Nature Nanotechnology* **7**, 11–23.

39. **Ahmad RK, Parada AC, Hudziak S, Chaudhary A and Jackman RB** (2010) Nanodiamond-coated silicon cantilever array for chemical sensing. *Applied Physics Letters* **97**, 093103-1–093103-3.

40. **Yao Y, Chen X, Ma W and Ling W** (2014) Quartz crystal microbalance humidity sensors based on nanodiamond sensing films. *IEEE Transactions on Nanotechnology* **13**, 386–393.

41. **Yu X, Chen X, Yu X, Chen X, Ding X and Zhao X** (2019) Flexible wearable humidity sensor based on Nanodiamond with fast response. *IEEE Transactions on Electron Devices* **66**, 1911–1916.

42. **Cassivi Y, Perregrini L, Arcioni P, Bressan M, Wu K and Conciauro G** (2002) Dispersion characteristics of substrate integrated rectangular waveguide. *IEEE Microwave Wireless Components Letters* **12**, 333–335.

43. **Salonen P and Rahmat-Samii Y** (2007) Textile antennas: effects of antenna bending on input matching and impedance bandwidth. *IEEE Aerospace and Electronic Systems Magazine* **22**, 18–22.

44. **Denisov SA, Sokolina GA, Bogatyreva GP, Grankina TY, Krasil'nikova OK, Plotnikova EV and Spitsyn BV** (2013) Adsorption and electrical properties of nanodiamond powders in the presence of water vapor. *Protection of Metals and Physical Chemistry of Surfaces* **49**, 286–291.

45. **Wang RLC, Kreuzer HJ, Grunze M and Pertsin AJ** (2000) The effect of electrostatic fields on an oligo (ethylene glycol) molecule: dipole moments, polarizabilities and field dissociation. *Physical Chemistry Chemical Physics* **2**, 1721–1727.

Chang-Ming Chen was born in Sichuan, China. He received his Ph.D. degree at the School of Physical Electronics, University of Electronic Science and Technology of China (UESTC). He is currently a professor in the College of Communication Engineering, Chengdu University of Information Technology (CUIT). His current research interests include microwave and millimeter-wave circuits and system.

Lu Chen was born in Sichuan, China. She received her BS degree from the School of Microelectronics and Solid-State Electronics, University of Electronic Science and Technology of China (UESTC), Sichuan, China in 2018. She received her MS degree from the School of Materials Science and Engineering, Beihang University (BUAA), Beijing, China in 2021. She is currently an assistant lecturer in the Chengdu Aeronautic Polytechnic. Her current research interests include microelectronics materials and devices.

Yao Yao was born in Sichuan, China. He received his BS degree from the School of Information Science and Technology, Southwest Jiaotong University (SWJTU), Sichuan, China in 2006. He received his Ph.D. degree at the Southwest Jiaotong University (SWJTU), Sichuan, China in 2013. He is currently an associate professor in School of Automation Engineering, University of Electronic Science and Technology of China (UESTC). His current research interests include carbon-based electronics and acoustic sensors.

Ye Peng was born in Sichuan, China. She is currently an associate professor in the Engineering Practice Center, Chengdu University of Information Technology (CUIT). Her current research interests include RF and microwave sensors.